WATER RESOURCES RESEARCH, VOL. 45, W05427, doi:10.1029/2009WR007731, 2009

Click Here for Full Article

Water velocity and the nature of critical flow in large rapids on the Colorado River, Utah

Christopher S. Magirl,[1] Jeffrey W. Gartner,[2] Graeme M. Smart,[3] and Robert H. Webb[2]

Received 13 January 2009; accepted 25 March 2009; published 28 May 2009.

[1] Rapids are an integral part of bedrock-controlled rivers, influencing aquatic ecology, geomorphology, and recreational value. Flow measurements in rapids and high-gradient rivers are uncommon because of technical difficulties associated with positioning and operating sufficiently robust instruments. In the current study, detailed velocity, water surface, and bathymetric data were collected within rapids on the Colorado River in eastern Utah. With the water surface survey, it was found that shoreline-based water surface surveys may misrepresent the water surface slope along the centerline of a rapid. Flow velocities were measured with an ADCP and an electronic pitot-static tube. Integrating multiple measurements, the ADCP returned velocity data from the entire water column, even in sections of high water velocity. The maximum mean velocity measured with the ADCP was 3.7 m/s. The pitot-static tube, while capable of only point measurements, quantified velocity 0.39 m below the surface. The maximum mean velocity measured with the pitot tube was 5.2 m/s, with instantaneous velocities up to 6.5 m/s. Analysis of the data showed that flow was subcritical throughout all measured rapids with a maximum measured Froude number of 0.7 in the largest measured rapids. Froude numbers were highest at the entrance of a given rapid, then decreased below the first breaking waves. In the absence of detailed bathymetric and velocity data, the Froude number in the fastest-flowing section of a rapid was estimated from near-surface velocity and depth soundings alone.

Citation: Magirl, C. S., J. W. Gartner, G. M. Smart, and R. H. Webb (2009), Water velocity and the nature of critical flow in large rapids on the Colorado River, Utah, *Water Resour. Res.*, *45*, W05427, doi:10.1029/2009WR007731.

1. Introduction

[2] Rapids occur in bedrock-controlled rivers where constrictions or drops in bed elevation accelerate flow to near-critical conditions, resulting in breaking waves, air entrainment, and a steepened localized water surface slope. Along the Colorado River and its major tributaries in the western United States, most rapids form in response to the collection of coarse-grained sediment at the mouths of tributaries [*Howard and Dolan*, 1981; *Webb*, 1996; *Grams and Schmidt*, 1999; *Webb et al.*, 2004], creating what has been termed the fan-eddy complex [*Schmidt and Rubin*, 1995]. Rapids in some reaches of bedrock-controlled rivers dominate the geomorphology along the river corridor, governing the nature of the river's drop in water surface elevation [*Leopold*, 1969], promoting the deposition and storage of sand on the channel margins [*Schmidt and Rubin*, 1995; *Hazel et al.*, 2006], and depositing coarse-grained bars and concomitant secondary rapids downstream [*Howard and Dolan*, 1981; *Webb et al.*, 1989; *Melis et al.*, 1994]. In addition to affecting morphology, rapids influence aquatic ecology by raising dissolved-oxygen levels in rivers and promoting biomass production on the coarse-sediment substrate beneath rapids [*Stevens et al.*, 1997]. Biologists speculate the native fish populations in the western United States evolved to survive the extreme velocity and turbulence of rivers with abundant fan-eddy complexes [*Douglas and Marsh*, 1996]. Rapids are also an important recreational resource for the public [*Loomis et al.*, 2005]. Despite their importance, scientific literature offers relatively little quantitative data on rapids.

[3] *Tinkler* [1997] used an electromagnetic current meter to measure flow in a fast-flowing, bedrock-controlled river in Ontario, and a number of researchers have made flow measurements in mountain streams [e.g., *Jarrett*, 1984; *Wohl and Thompson*, 2000; *Thompson*, 2007; *Wilcox and Wohl*, 2007]. *Kieffer* [1987, 1988] was one of the first to attempt systematic measurements of velocity in rapids in a large river. Using a calibrated video camera and floating tracer particles, Kieffer recorded the movement of particles through large rapids in the Colorado River to measure, in a Lagrangian frame of reference, velocity along trace lines reporting velocities as large as 10 m/s. However, floating particles only measure the velocity at the water surface offering little insight into the subsurface mechanics. Flow velocity data throughout the water column are needed, for example, to analyze shear stresses on the bed, verify numerical models, and calculate the flow regime in rapids.

[4] Controversy also surrounds the issue of Froude number, *Fr*, in rapids, with some researchers reporting or postulating supercritical flow and *Fr* above 1.0 within rapids [*Kieffer*, 1985, 1990; *Miller*, 1994] and other researchers

[1]U.S. Geological Survey, Tacoma, Washington, USA.
[2]U.S. Geological Survey, Tucson, Arizona, USA.
[3]National Institute of Water and Atmospheric Research, Christchurch, New Zealand.

This paper is not subject to U.S. copyright.
Published in 2009 by the American Geophysical Union.

speculating flow in even high-gradient streams with moveable beds remains critical or subcritical, rarely achieving or sustaining supercritical conditions [*Jarrett*, 1984; *Trieste*, 1992; *Grant*, 1997; *Parker and Izumi*, 2000]. *Jarrett* [1984] found that, despite high velocity and extreme turbulence, flow in mountain streams is critical or subcritical, leading to the assumption that supercritical flow in natural streams does not exist for any extended lengths. *Tinkler* [1997] documented critical *Fr* in the fastest section of the channel with no pronounced regions of supercritical flow. Tinkler also showed that the region of critical flow expanded spatially with increasing discharge, but that the flow did not transition to supercritical. *Tinkler* [1997] theorized that while supercritical flow was possible, flows in most natural channels were no faster than critical or just slightly supercritical. More importantly, Tinkler recognized and explained how threads of near-critical flow in the fastest current could coexist with subcritical flow near the shoreline, a channel condition earlier analyzed by *Blalock and Sturm* [1981]. *Grant* [1997] offered the more general hypothesis that flow in channels with a moveable bed is predominantly subcritical. Nonetheless, perceptions persist within the research community that flow in large rapids is supercritical. *Kieffer* [1988] reported supercritical *Fr* for a number of Grand Canyon rapids at discharges below 500 m^3/s. For example, *Kieffer* [1988] stated the maximum *Fr* was 2.4 at Lava Falls Rapid and 2.3 at Dubendorff Rapid; Kieffer also stated the region of supercritical flow in the core of Dubendorff Rapid extended roughly 250 m from the tongue of the rapid to the tailwaves.

[5] Knowledge of flow regime in rivers is important for accurate analysis of the hydraulics and geomorphology of the fan-eddy complex. For example, *Carling* [1995] demonstrated that in a bedrock channel, boulder bar deposits form immediately downstream from hydraulic jumps, a morphologic feature that depends on the presence of depth-integrated supercritical flow. Also, with the advancement of numerical modeling of rivers, assumptions of the flow regime is required to produce accurate and realistic results.

[6] Even fundamental topologic data for rapids, consisting of bathymetry and water surface topography, are generally unavailable. *Kieffer* [1987] reported limited bathymetry data for rapids on the Colorado River, and *Thompson et al.* [1999] and *Valle and Pasternack* [2006] collected detailed water surface topographic data and bathymetry in mountain streams. *Thorne and Zevenbergen* [1985] surveyed the water surface along the shoreline of high-gradient mountain streams. Several researchers have reported the water surface profile of rapids surveyed along the shoreline [e.g., *Grams and Schmidt*, 1999; *Webb et al.*, 1999; *Larsen et al.*, 2004; *Yanites et al.*, 2006]. But the water surface profiles measured along the shoreline and through the middle of the rapid may be different, and accurate measurement of the slope of the water surface profile is needed for sediment transport studies within rapids.

[7] The present study measured water velocity, water surface topology, and bathymetry within three large rapids on the Colorado River in eastern Utah. Two flow-measurement instruments were employed to quantify the mechanics of hydraulics in rapids. The first of these instruments is an electronic pitot-static tube designed for swift-water measurements. This instrument, known as the pressure operated electronic meter, was developed by *Smart* [1994, 1999] to measure velocity and turbulence in swift mountain streams. *Nikora and Smart* [1997] used the pitot tube to characterize turbulence, velocity, and velocity structures for a number of fast-flowing gravel bed rivers in New Zealand. Similarly, *Ackerman and Hoover* [2001] used a Preston-static tube (i.e., a pitot tube near a fixed boundary) to measure water velocity and shear stress in shallow mountain streams. The second instrument is an acoustic Doppler current profiler (ADCP). Used for making discharge measurements and determining velocity profiles in alluvial rivers [*Yorke and Oberg*, 2002], the ADCP has the ability to measure velocities throughout the vertical water column and simultaneously record bathymetry. For the first time, the collection of a complete data set of bathymetry and water velocity throughout the water column in large rapids allowed the calculation of *Fr*, enabling a comparison with earlier estimates of *Fr* in rapids [*Kieffer*, 1988]. More importantly, these new data offer insight into the nature of hydraulics in rapids with the promise to aid future numerical and empirical studies.

2. Methods

2.1. Terminology

[8] For the purpose of this study, a rapid is defined as any continuous section of river where breaking waves caused by the acceleration of flowing water from a constriction or drop in bed elevation spans the width of the channel. In terms of boating, a feature is typically considered a rapid when the waves are large enough to impede navigation. The section of river above the rapid is often a deep, relatively slow-moving, shallow-gradient reach known as the upper pool. The water accelerating into the rapid is bounded by breaking waves extending laterally in from the shore. This fast, smooth water at the rapid's entry is known as the tongue of the rapid, and the high-gradient section of the rapid below the first breaking waves is the core of the rapid. Farther downstream, the reach of transient breaking waves in the decelerating flow is termed the tailwaves section. Details of the components and terminology of a rapid can be found in work by *Leopold* [1969] and *Kieffer* [1990]. Consistent with convention, the left and right shoreline are named with respect to the observer facing downstream.

2.2. Site Selection

[9] Flow, water surface, and bathymetric measurements were made in the Colorado River within Cataract Canyon from 23 to 26 April 2006. Cataract Canyon is within Canyonlands National Park, just below the confluence of the Green and Colorado rivers in eastern Utah (Figure 1). While flow regulation from upstream damming affects the flood regime in Cataract Canyon, the Colorado River at this location is still subject to large spring snowmelt floods, heavy sediment load, and seasonal temperature fluctuations characteristic of a free-flowing river [*Webb et al.*, 2004]. Cataract Canyon, containing more than 27 extant rapids over a 21 km reach, is popular with white-water enthusiasts. These rapids are numbered sequentially in the downstream direction: rapids 1 and 27 are 6.8 and 26.1 km downstream from the confluence, respectively [*Belknap et al.*, 2006]

[10] Two sections of river were measured and analyzed in detail for this study. The first section consists of a series of closely spaced rapids starting with rapid 13, formed by a

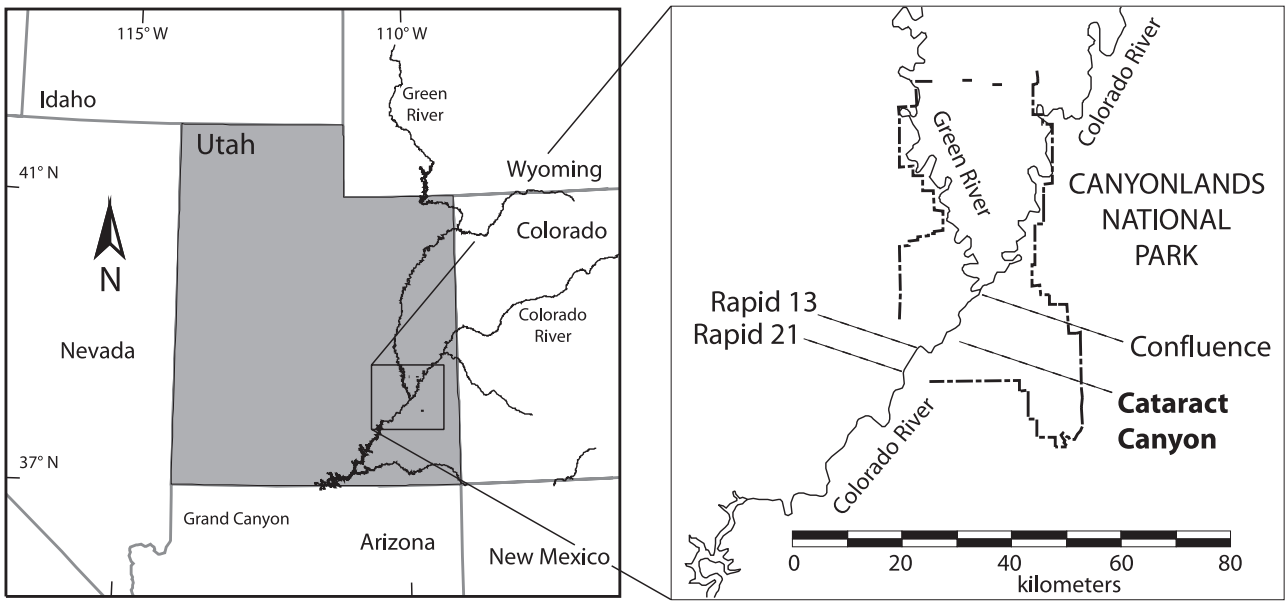

Figure 1. Map of Colorado River in Cataract Canyon, Utah, showing the location of the rapids measured in this study.

debris fan at the mouth of Range Canyon, 18.7 km below the confluence (Figure 2). River width varied from 60 to 130 m through this section of river at the measured discharge, and the rapids were not difficult to ascend with a powered boat. Flow measurements (both pitot tube and ADCP) were made throughout rapid 13 and rapid 14, and water surface profile data were collected from rapid 13 to below rapid 15. The second section of river studied was at rapid 21, created by a debris fan issuing from Teapot Canyon, 22.2 km below the confluence (Figure 2). This second site was chosen because it represents, in contrast to rapid 13, one of the larger, more navigationally challenging rapids on the river. River width varied from 65 to 95 m through this section of river at the measured discharge. Because of time constraints and difficulties receiving a global positioning system (GPS) signal with the ADCP, only pitot tube measurements were collected at rapid 21.

[11] The discharge in the Colorado River during data collection, calculated using flow data provided by the Colorado Basin River Forecast Center (B. Reed, Colorado Basin River Forecast Center, written communication, 2007) and corrected with an in situ discharge measurement using the ADCP, fluctuated between 607 and 676 m^3/s. On the basis of available discharge records from 1884 to 2006, the estimated 2-year recurrence interval flood in Cataract Canyon is 1650 m^3/s and the 10-year flood is 3020 m^3/s [*Webb et al.*, 2004]. While the discharge values during this study were not exceptional, they are significant: a discharge in Cataract Canyon of 607 m^3/s is exceeded, on average, only about 20% of time. The ADCP showed bed load was active during measurements, though neither the bed load nor suspended load adversely affected bathymetric or velocity measurements.

2.3. Tacheometry and Bathymetry

[12] All measurements were made from a 5.5 m boat designed to navigate rapids. The boat had a catamaran design with two 6 m inflatable tubes providing buoyancy and a rigid aluminum frame provided structural support and a working platform. A pivoting boom attached to the aluminum frame at the front of the boat provided the means to deploy each flow measurement instrument. Details of the boat and the design of the instrument boom are available in work by *Magirl* [2006].

[13] A 360° mirrored prism mounted to the top of the boom assembly allowed the position of the boat to be surveyed with a total station positioned on shore; surveyed ground points along the shoreline were also collected. The total station was placed on a prominent point above the river providing its operator an unobstructed view of boat operations and the shoreline. The positional error of the surveyed boat location, affected by boat movement during the survey shot, was estimated to be about ±15 cm in three dimensions. The positional error of a surveyed ground point using rod and prism, given the uneven surface of debris fans and the ambiguity of the survey feature (e.g., a surging shoreline), was typically on the order of 3–5 cm in three dimensions.

[14] Viewed in profile, the shape of the water surface through a rapid was approximated by fitting a regression curve to the available water surface data. The regression used a hyperbolic tangent function of the form

$$h = -a\tanh(m(x-c)) + b, \tag{1}$$

where h is the interpolated water surface elevation, x is the downstream distance through the rapid, and a, m, c, and b are correlation constants chosen to minimize the sum of the residuals during the regression. The water surface profile through rapids is not linear but tends to be sinuous [*Yanites et al.*, 2006] and is well approximated with a hyperbolic tangent function. Equation (1) offered an objective way to determine the slope of the water surface through the rapid by taking the first derivative of the best fit model; positive slope indicated a drop in the river's water surface elevation. Considering the positional error of the survey points, and considering a worse case of error propagation, the uncertainty of the slope calculation was about 20%.

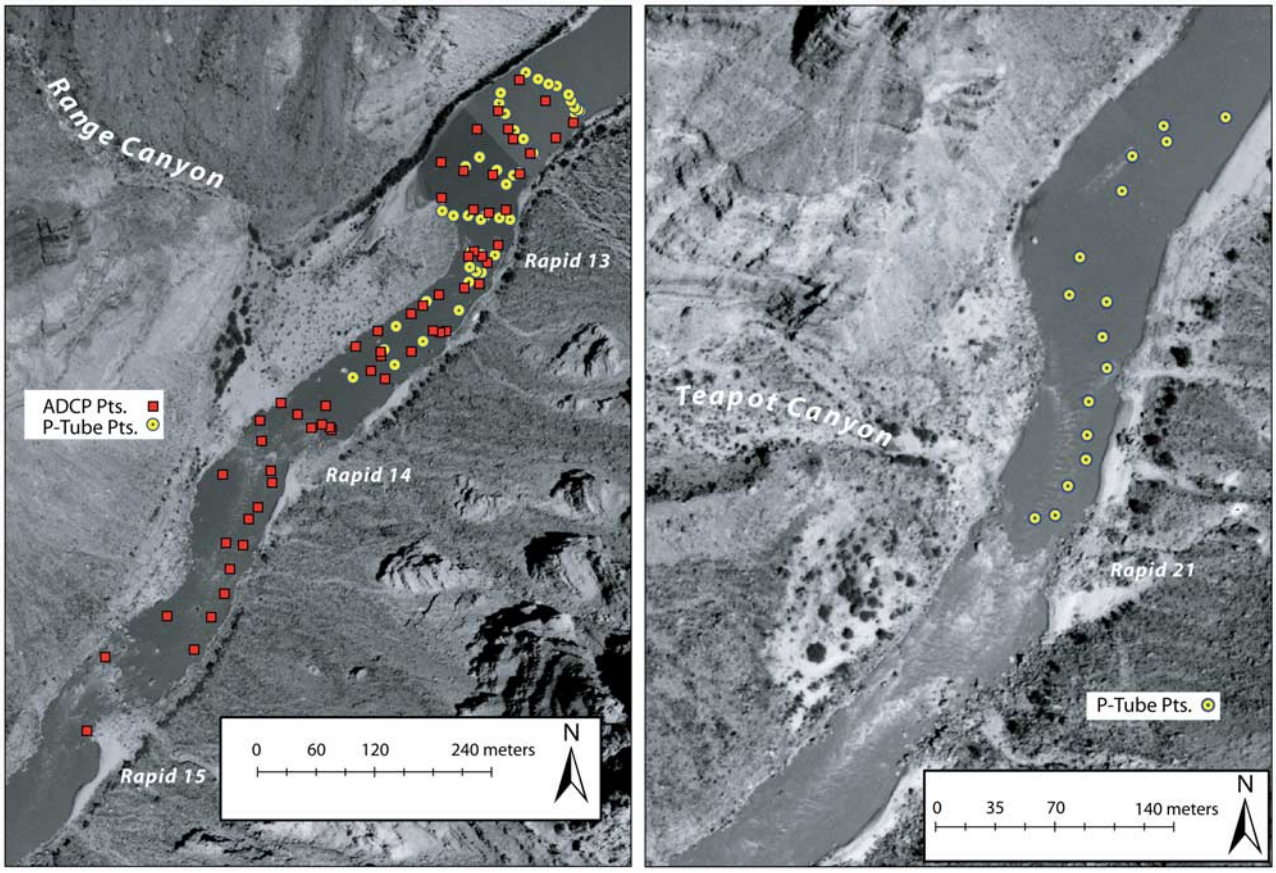

Figure 2. Aerial photographs of the Colorado River in Cataract Canyon, Utah, at a discharge of about 120 m^3/s. (left) Section of the river near Range Canyon showing rapids 13, 14, and 15. ADCP and pitot tube measurements were made above and below rapids 13 and 14. (right) Section of the river at Teapot Canyon, the tributary forming rapid 21. Fifteen pitot tube measurements were made along the thalweg from the upper pool to the tongue of the rapid, just upstream of the first breaking waves.

[15] Bathymetric data were collected with two instruments. Mounted to the rear of the boat was a Lowrance X59DF dual-frequency fathometer. (Use of trade or brand names in this paper is for identification purposes only and does not constitute endorsement by the U.S. Geological Survey.) Depths displayed by the fathometer from each location were recorded in a field book then later tied into the survey. Details of the fathometer were documented by *Magirl et al.* [2006]. The ADCP, mounted on the boom assembly at the front of the boat, also recorded bathymetry. Rather than using the depth average of the four ADCP beams reported by the instrument, a process that tends to integrate and average features on the river bed, point depth data from each beam for a given ADCP ping ensemble were calculated individually using AdMap software (D. S. Mueller, U.S. Geological Survey, written communication, 2007). AdMap uses the instrument pitch, heading, roll, and GPS-calculated position to rectify the depth sounding from an individual beam into three-dimensional space. Details of the technique used to improve bathymetric data at rapids 13 and 14 using AdMap are available in work by *Magirl et al.* [2007].

[16] Tacheometric surveying of boat position, combined with water surface data measured along the river's shoreline, enabled the construction of a three-dimensional representation of the water surface for a given section of river. To our knowledge, this is the first time the three-dimensional water surface of a large rapid has been directly measured and reported. Combined with the bathymetric data, this three-dimensional water surface allowed the characterization of the complete topologic domain of the water in the rapid (i.e., the water surface, shorelines, and bathymetry).

2.4. Flow Measurement Dwell Time

[17] When making velocity measurements, the operator attempted to hold the boat in a static, upstream facing position in the river for 60 s, allowing the averaging of 1 min of continuous flow measurements. It was not known, a priori, what measurement dwell time was needed to fully average all turbulent fluctuations in the flow; 60 s was used. Analysis of the velocity data collected with the pitot tube indicated that in the fastest section of rapid 21, 60 s was just long enough to capture and average all the turbulent fluctuations. Ideally, a total dwell time of 120 s would better characterize the fastest flows and should be used in similar studies in the future. Nonetheless, for the purposes of this study, a 60 s dwell was adequate for each measurement, particularly for the slower-flow measurements.

[18] On the basis of GPS data used by the ADCP for positional tracking, the boat drift around the target position during a given measurement was estimated to be on the order

of ±5 m (horizontally) in the fastest, most turbulent sections of the river. Therefore, the velocity data collected with each instrument could have come from locations in the river up to 5 m away from the surveyed boat location. This positional accuracy of the flow measurement location improved in slower water.

2.5. Flow Instrumentation

[19] The electronic pitot-static tube used in the study was designed and built at New Zealand's National Institute of Water and Atmospheric Research. This instrument has dynamic and static pressure sensing ports similar to aircraft airspeed and altitude sensors. The pitot tube is mounted at the front of a streamlined "torpedo" to reduce vibration of the pressure sensors. The dynamic pressure port at the tip of the tube is 3 mm in diameter. The static pressure sensing port comprises a ring of eight 1 mm holes equally spaced around the 16 mm diameter shaft of the pitot tube. Static and dynamic pressures are measured with Motorola MPX100 series transducers with ±0.25% linearity and response time of 1×10^{-3} s. Measuring the difference between the oncoming flow's stagnation pressure and static pressure allows Bernoulli's principle [*Fox and McDonald*, 1985] to be used to estimate the scalar component of the free-stream velocity. The instrument was designed to measure flow velocity up to 9 m/s.

[20] The pitot tube measures pressure which is directly proportional to velocity head,

$$\frac{u_i^2}{2g}, \tag{2}$$

where u_i is the instantaneous velocity measurement and g is the gravitational constant. A high sampling frequency is required to correctly calculate mean velocity in turbulent flow, where $\overline{u_i} \neq \sqrt{\overline{u_i^2}}$. The instrument sampling frequency (28 Hz) enabled the pitot tube to measure even the smallest turbulent fluctuations within the flow [*Smart*, 1999]. Unlike turbulence measurements with an acoustic Doppler velocimeter [*Lane et al.*, 1998], the pitot tube required no signal processing or active filtering of the output signal because the pitot tube directly measured the pressure fluctuations in the flow.

[21] The electronic pitot tube was mounted 0.39 m below the water surface and attached to the end of the boom assembly with a pivoting steel rod. Deeper measurements in the water column were not attempted out of safety concerns for the crew and instrument. The pivot of the rod (roughly ±15° around an axis parallel to the boom rotation axis) allowed the streamlined pitot tube to self-adjust its angle of attack to the oncoming flow, thus more accurately quantifying the scalar component of oncoming flow. Velocity components orthogonal to the axis of the pitot tube, from instrument misalignment or turbulent eddies sweeping past the instrument ports, have the potential to induce measurement error. *Ackerman and Hoover* [2001], however, found velocity measurements were reasonably consistent for a pitot-static tube oriented at angle of attacks up to ±20°. The magnitude of error from orthogonal velocity components in the flow was not evaluated for this study, though this error source was probably small.

[22] The ADCP, a Teledyne RD Instruments 600 kHz WorkHorse unit with a Trimble AG132 differential GPS, was used to measure water velocity profiles. The ADCP's theory of operation is well documented [e.g., *RDInstruments*, 1996; *Yorke and Oberg*, 2002; J. W. Gartner and N. K. Ganju, A preliminary evaluation of near-transducer velocities collected with low-blank acoustic Doppler current profiler, paper presented at Hydraulic Measurements and Experimental Methods 2002, American Society of Civil Engineers, Estes Park, Colorado, 28 July to 1 August 2002]. ADCPs determine water current velocity by emitting sound waves, or pings, at known frequency and measuring the Doppler shift of the returning sound waves reflected from particles suspended in the moving water. Using an array of four acoustic transducers oriented 90° apart and 20° from the vertical (Janus configuration), and by range gating the acoustic returns, the ADCP calculates the magnitude and direction of water moving at discrete depths or bins. Separate bottom-track pings are also used to sound bathymetric depth.

[23] The ADCP was set to sample using water mode 1 [*RDInstruments*, 1996] with a 0.25 m blank distance and 0.50 m bin size. Water mode 1 is robust, designed to operate in flows with high shear, turbulence, and velocity up to 10 m/s. For this study, two water profile pings and three bottom-track pings were selected to make up a measurement ensemble. An ensemble represents the averaging of multiple pings to determine both velocity and water depth. The sampling rate for an ensemble was approximately 1 Hz.

[24] In calculating velocity, an ADCP assumes the flow in the water column is homogeneous at a given bin (height) in the water column. This assumption may lead to errors when measuring potentially three-dimensional flow structures within the rapid.

[25] Also, the high velocity, aeration, and extreme turbulence in the rapid required a relatively deep ADCP placement of 0.69 m below the water surface. Even with this instrument depth, some ensembles were missing, particularly in fast or turbulent regions of the river. Data losses, caused by attenuation of signal due to suspended sediment, loss of instrument bottom track, low signal correlation, air bubbles entrained in the flow under the instrument, or perhaps trapped air bubbles on the transducers, were probably the source of most ADCP reliability issues. The percentage of missing ensembles was reported as a proxy for relative instrument effectiveness at a particular location.

[26] Deeper placement of the ADCP, however, meant the instrument would not measure velocity within one meter of the surface. Having no other options while working with ADCP data, the water velocity within one meter of the surface was estimated to be equivalent to the velocity measured in the top bin, an assumption later shown to potentially invalid in the faster sections of the rapid. Nevertheless, in lieu of having no other available information, it was the best assumption available.

[27] Another issue with working in bedrock canyons was the problematic reception of the GPS receiver, which was needed when moving-bed conditions created measurement bias for the ADCP using bottom tracking. For example, no ADCP data were collected at rapid 21 because of insufficient GPS coverage. Fortunately, the GPS did work long enough in the canyon setting at rapids 13 and 14 to provide useful data.

2.6. Froude Number

[28] Froude number, *Fr*, compares inertial and gravitational forces within a flow. As long as vertical velocities are small and the pressure distribution is hydrostatic, it is the ratio of water velocity to the propagation velocity of a shallow water wave. Froude number is typically calculated with velocity averaged throughout the cross section [e.g., *Chow*, 1959]. Because of the nature of the flow measurements collected in this study, local *Fr* was calculated using the approach outlined by *Liggett* [1993] using shallow-water theory,

$$Fr = \frac{\overline{u}}{\sqrt{g\eta / \beta}}, \tag{3}$$

where $\overline{u}$ is depth-integrated velocity. The total depth of flow is given by η. The nonuniform velocity distribution coefficient, β, is given by

$$\beta = \frac{\int_0^\eta u^2 dz}{\overline{u}^2 \eta}. \tag{4}$$

Velocity, $u(z)$, is a function of height above the bed of the river as measured with the ADCP. An important assumption behind the derivation of equation (3) is that the flow has a hydrostatic pressure distribution with negligible vertical accelerations. In highly three-dimensional flow, or in flow with a deformed free surface and significant vertical velocities, equation (3) is not applicable and the usual definition of *Fr* is called into question.

[29] In the absence of velocity profile data (e.g., ADCP-collected velocity data from the entire water column), *Fr* can be estimated if near-surface velocity and water depth are known. An assumption is made that the depth-integrated mean velocity in the water column is 85% of the surface velocity, u_s [*Rantz et al.*, 1982; *Costa et al.*, 2000]. This is a reasonable assumption if the velocity profile is logarithmic. Assuming a value of β, *Fr* can then be estimated as follows:

$$Fr = \frac{0.85 u_s}{\sqrt{g\eta / \beta}}. \tag{5}$$

In an attempt to confirm the validity of the *Fr* calculations obtained by equations (3) and (5), a simplified approach to calculating *Fr* was also applied. If flow in a rapid was approximately one dimensional, then detailed bathymetric data measured during the study could be used to estimate *Fr*. According to *Henderson* [1966, p. 51], *Fr* in an irregular, low-gradient channel with steady, one-dimensional flow is given by

$$Fr = \sqrt{\frac{Q^2 B}{g A^3}}, \tag{6}$$

where Q is discharge, B is the top width of the water surface, and A is the cross-sectional area of the flowing water. While the high-velocity, three-dimensional flow conditions within rapids makes the application of equation (6) inappropriate in general, the equation can be used as a first-order check of the validity of *Fr* as calculated with equations (3) and (5). By setting $Fr = 1$, equation (6) can also be used to calculate critical depth of given cross section for a known discharge. If the critical depth falls below the measured depth in the river, the flow is subcritical. Inversely, if the critical depth lies above the measured depth, flow is supercritical. *Schmidt* [1990] used the approach of equation (6) to calculate *Fr* in Badger Rapid in Grand Canyon.

3. Results and Discussion

3.1. Water Surface Profile and Bathymetry

[30] A topographic map of rapids 13, 14, and 15 was assembled using 101 water surface elevation points collected during flow measurements and 82 survey points from the water's edge (Figure 3b). The slope of the water surface, calculated using equation (1), shows the relatively low-gradient drop in rapid 13, the steeper gradient of rapid 14, and the relatively high-gradient drop of rapid 15 (Figure 3c). A secondary rapid is present between rapid 14 and rapid 15, formed by a deposit of coarse-grained sediment carried down from rapids 13 and 14. These secondary rapids are a common geomorphic characteristic of rivers with fan-eddy complexes [*Howard and Dolan*, 1981; *Webb et al.*, 1989; *Melis et al.*, 1994; *Grams and Schmidt*, 1999].

[31] The bathymetric map of rapids 13 and 14 (Figure 3d) was assembled using over 15,000 ADCP depth measurements processed with AdMap software. Even in the turbulence of rapids, ADCP bottom pings were reliable and did not require the averaging of multiple measurement ensembles.

[32] Viewed in profile, the hydraulic characteristics of rapids 13, 14, and 15 are apparent (Figure 4). Rapid 13 was a relatively long, low-gradient rapid with a total fall in elevation of just over 1.0 m and maximum slope of 0.006. Rapid 14 fell in elevation about 1.5 m and had a maximum slope of 0.02. In contrast, rapid 15, the largest of the three rapids in this reach, dropped about 2.0 m with a maximum slope of 0.03.

[33] The channel invert is also shown in Figure 4; this trace was constructed using the bathymetry data shown in Figure 3d. Mounds of alluvial material on the river bed that form the rapids are apparent, and total change in elevation of the river bed along 700 m of channel from rapid 13 to just above rapid 15 was less than 4 m affirming observations of *Webb et al.* [2004] that rapids 13–18 are subsections of one continuous rapid.

[34] The channel invert and water surface data measured at rapid 21 are plotted in Figure 5. Rapid 21 had a small riffle with less than 1.0 m drop just upstream of the main rapid. The main part of rapid 21 fell over 2.0 m. The trace of the invert showed the collection of coarse-grained alluvium deposited from Teapot Canyon is about 5 m below the water surface.

[35] Evident in the water surface maps are regions where the water surface along one shoreline was noticeably different from the water surface measured on the opposite shoreline or in the center of the channel. For example, the right shoreline in the pool below rapid 14 was 0.4 m above

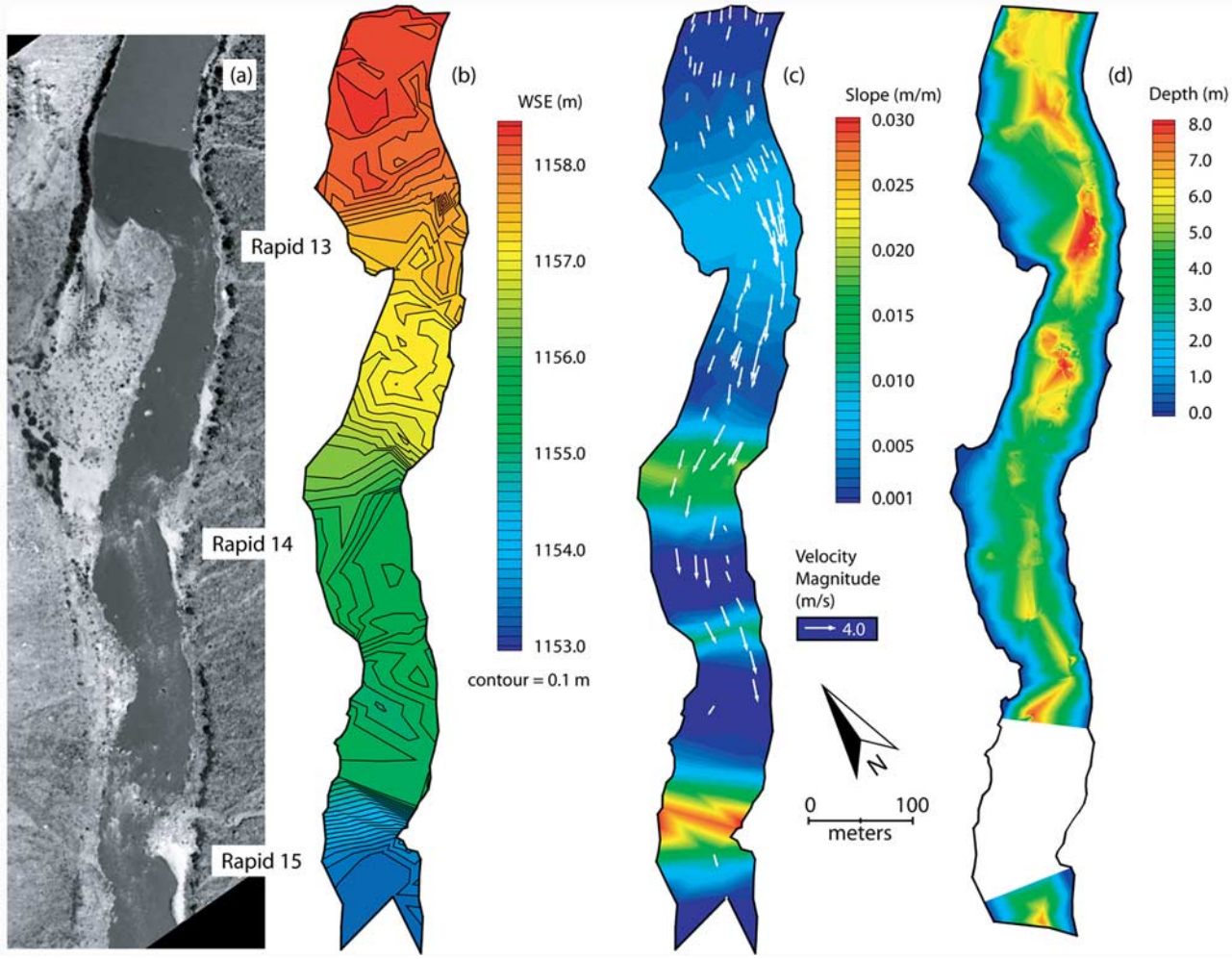

Figure 3. Topography near rapid 13 in Cataract Canyon, measured at a discharge of about 630 m^3/s: (a) aerial photograph of the river, (b) topography of the water surface, (c) contour map of the slope of the water surface with an overlay of velocity vectors from the pitot tube and from bin 1 of the ADCP measurements, and (d) the bathymetry map.

the shoreline on the left bank (Figure 4); similarly, the left shoreline of the pool below rapid 21 was 0.8 m above the shoreline across the river (Figure 5). These areas of super elevation are created by curvature of the river forcing the high-velocity flow exiting the rapid onto a downstream shore. Curvature of rapid 14 also caused significant differences in slope along the left shoreline versus the right shoreline.

[36] Even if the rapid had no curvature, water surface slope along the shoreline of a rapid was steeper than the water slope in the middle of the channel. Pooling along the shore above the rapid and sometimes strong recirculation eddies below the rapid can create a steep gradient on the shoreline with comparative shallow gradient down the main channel. For example, the water surface slope measured at rapid 14 was much different depending on the data used. The value of slope of 0.02 shown in Figure 4 was calculated using both shoreline and boat-based survey points. If only shoreline data from the left shoreline were used in the calculation, the computed slope would have been 0.045, twice as steep as the value incorporating water surface data. Thus measurements of water surface slope made exclusively using shoreline elevations overestimated the magnitude of the slope of the water surface in the rapid. *Magirl* [2006] found similar water surface slope behavior in rapids in Grand Canyon. Measurements made directly in the river, coupled with shoreline measurements, offered the most accurate way to calculate the water surface slope.

3.2. Pitot Tube Velocity Data

[37] The maximum mean velocity of 38 pitot tube measurements collected in rapid 13 was 4.3 m/s (Figure 6). Several measurements made within the upper pool yielded velocities between 1.5 and 2.0 m/s. As the river was constricted by the debris fan from Range Canyon, flow accelerated into rapid 13 and velocities rose to 4.1 m/s. Within the core of rapid 13, two groups of measurements were collected: data were collected along the area of fast water near the left shoreline and four additional measurements were made in a region of turbulent upwelling near the right shoreline. This region of upwelling is located downstream of the lateral waves and a strong eddy fence (i.e., a vertical boundary of pronounced velocity shear [*Schmidt and Graf*, 1990; *Best and Roy*, 1991; *De Serres et al.*, 1999; *Roy et al.*, 1999]) on

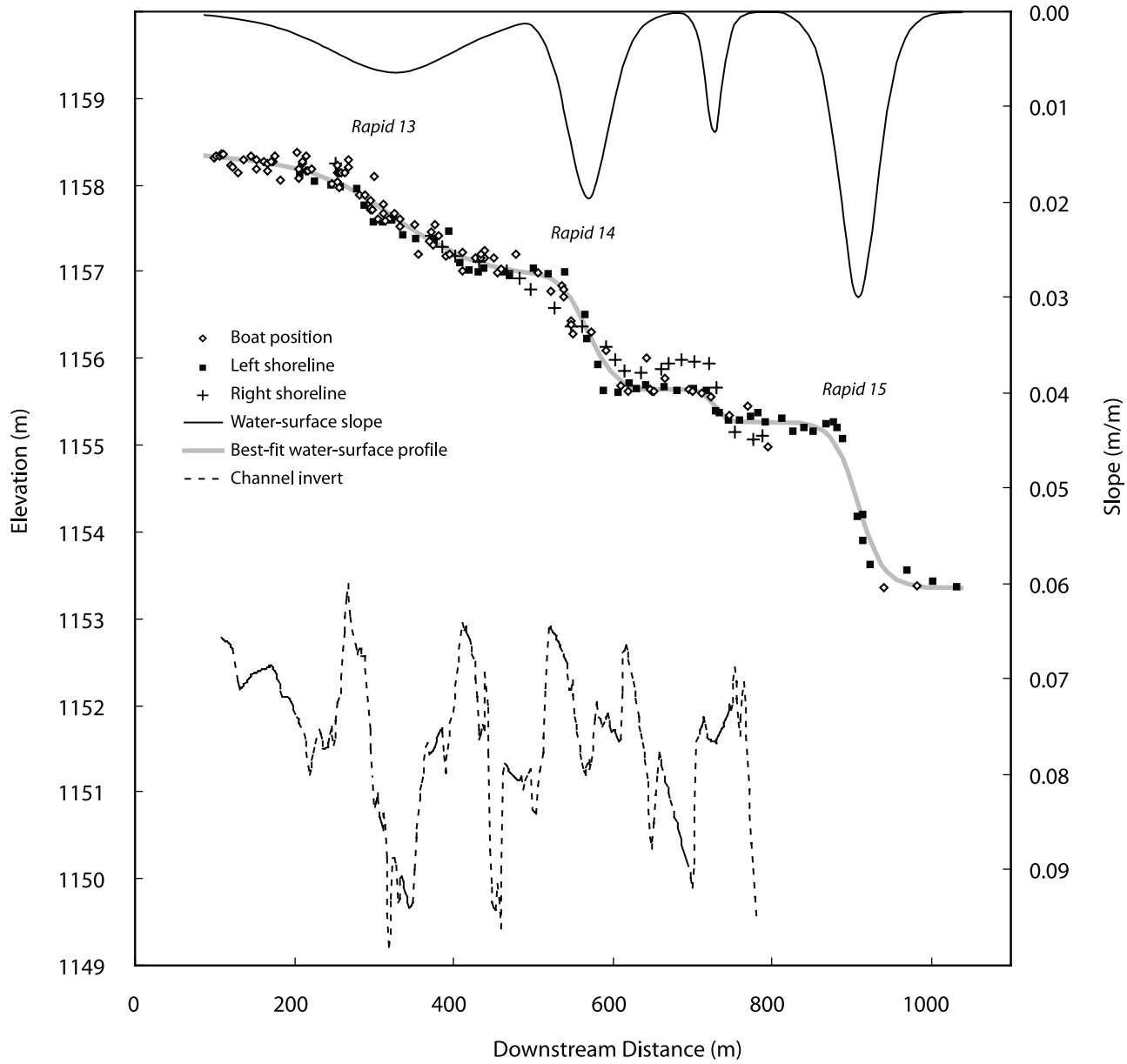

Figure 4. Longitudinal water surface profile of the Colorado River near rapid 13. Survey elevations were measured along the left shoreline and right shoreline and on the water surface. The channel invert (deepest part of the channel) is shown as well as the water surface profile modeled with equation (1). The water surface slope is shown on the second ordinate.

river right separating the fast water in the tongue from the slower water near the shore. This section of the river is best described as a boil train, a section of strong, turbulent upwelling and relatively slow surface velocities in the wake of the eddy fence.

[38] Along with the mean velocity, the complete range of instantaneous velocity measurements is displayed as offset bars in Figure 6. This range of velocity illustrates the magnitude of turbulent fluctuations at a given location in the river; overall velocity fluctuations were much larger in the core of the rapid than in the upper pool or the tongue indicating strong turbulence and energy dissipation. For rapid 13, the maximum measured velocity did not occur at the location of the steepest slope in the rapid. Instead, the highest mean velocity of 4.3 m/s was located slightly downstream from the area of steepest slope. The largest instantaneous velocity of 5.7 m/s was also recorded at this point.

[39] While no pitot tube measurements were collected in rapid 14, fifteen measurements were collected from the upper pool and tongue of rapid 21; dangerous and turbulent flow conditions precluded the collection of flow data in the core of rapid 21. Figure 7 shows the mean velocity 0.39 m below the water surface of the upper pool was generally decreasing from 2.7 to 2.0 m/s, moving downstream. At a downstream distance of about 160 m, near-surface velocity began to accelerate into the upper riffle of rapid 21 reaching values greater than 4.0 m/s. The flow then entered the main part of rapid 21; two measurements were taken within the tongue of the main section of the rapid showing accelerating

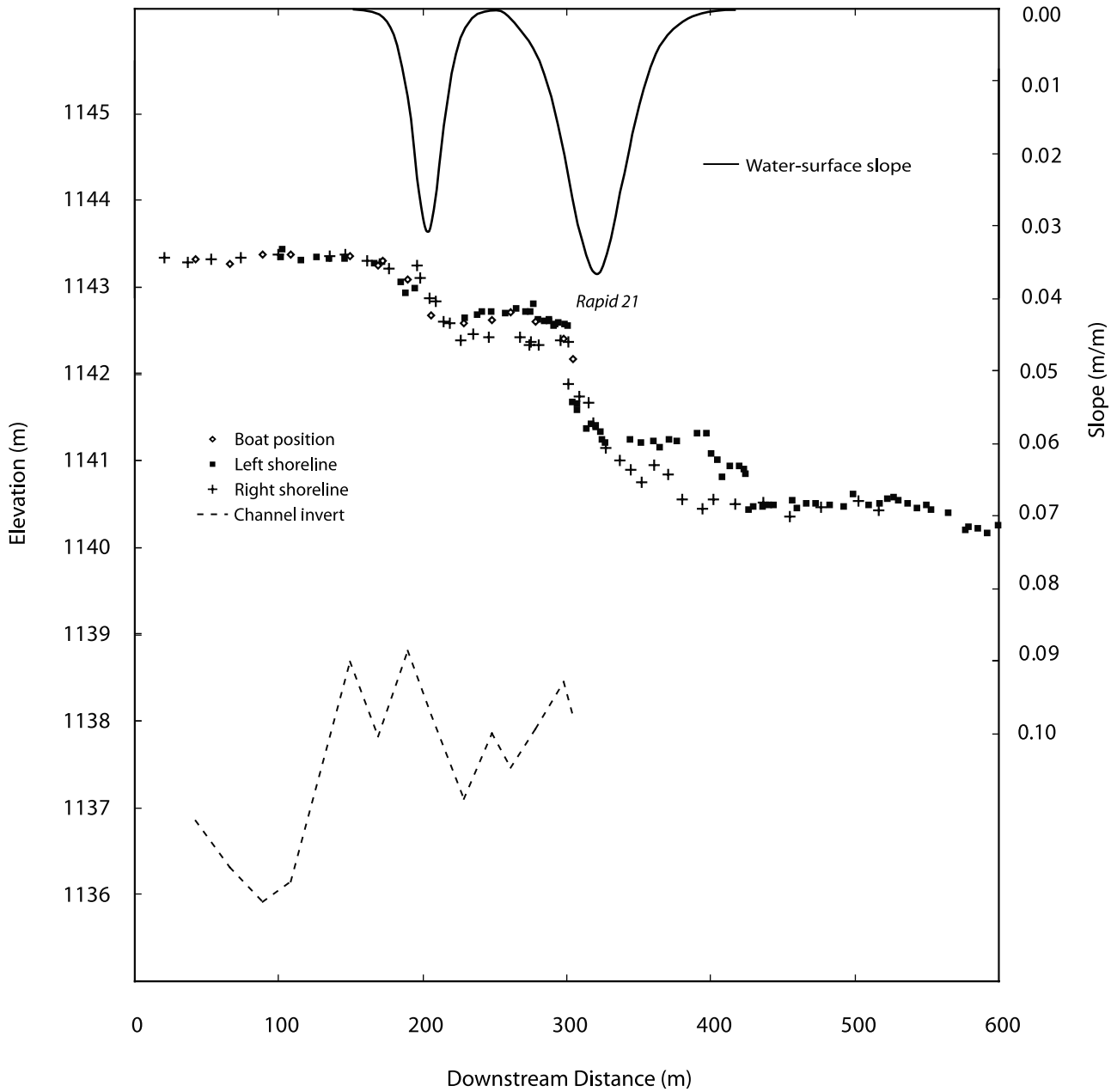

Figure 5. Longitudinal water surface profile of the Colorado River near rapid 21. Survey elevations were measured along the left shoreline and right shoreline and on the water surface. The channel invert and the slope are also shown.

near-surface velocity and a maximum average velocity of 5.2 m/s. The largest instantaneous velocity measured was 6.5 m/s.

3.3. ADCP Data

[40] During two measurement sessions, 63 velocity profile measurements were made with the ADCP at dwell points through rapids 13 and 14. The highest mean velocity measured at rapid 13 was 3.4 m/s in ADCP bin 1, at a depth of 1.55 m below the water surface. The highest mean velocity measured at rapid 14 was 3.7 m/s, also in bin 1. Some fast water in the core of each rapid, however, was not directly measured. In rapid 13, water accelerated by the constriction pushed along the left shoreline. Waves and rocks in this fast-water section created safety concerns for boat operation, thus preventing measurements. Visually, this water was estimated to be about 10% faster than the measured flow. Where ADCP data were collected, velocity generally decreased with depth in the water column. The direction of flow for a given measurement site was usually uniform throughout the water column though some locations, particularly in the rapids and recirculation eddies, exhibited changing flow directions with depth in the water column, reflecting the complex nature of flow fields in rapids.

[41] As expected, instrument performance was good in the slower water of the upper pool with the percentage of missing ensembles remaining below 25%. The performance of the instrument was mixed in the faster water of rapids 13

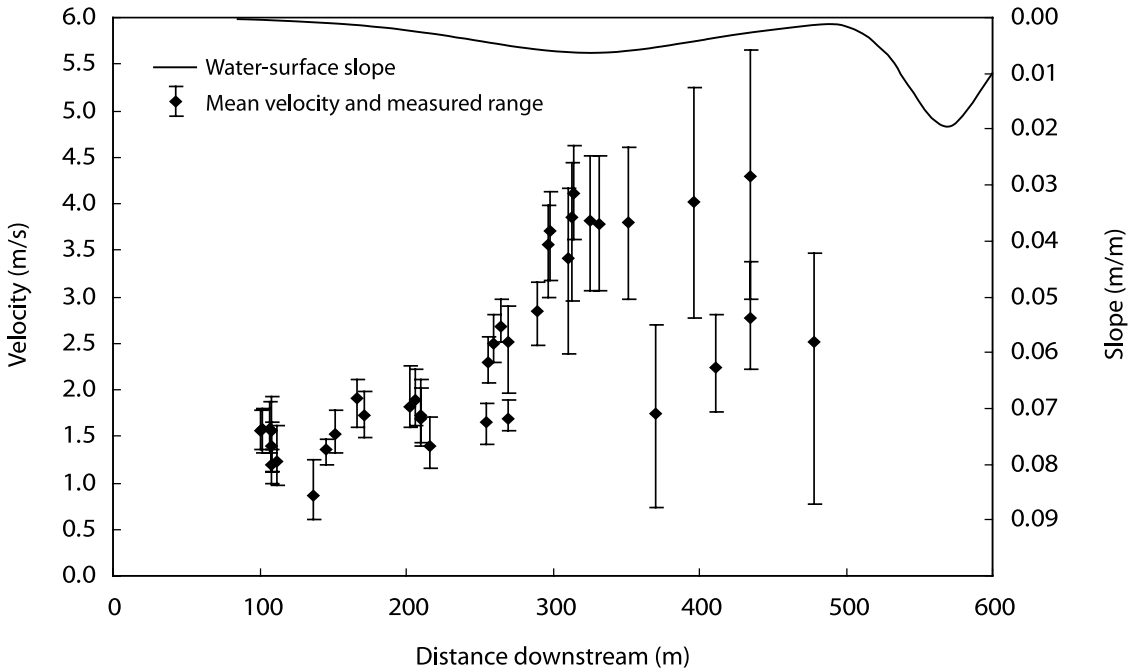

Figure 6. Pitot-static tube measured mean velocity at rapid 13. The slope of the rapid is also shown on the second axis. The tongue of the rapid was located at a downstream distance of 300 m. Error bars on the velocity data show the range of instantaneous velocities recorded by the pitot tube during a given measurement. The maximum mean velocity at rapid 13 was 4.3 m/s, and the maximum recorded instantaneous velocity was 5.7 m/s.

and 14 with missing-ensemble rates ranging between 14% and 73%. High percent of missing ensembles does not necessarily indicate poor velocity data by the ADCP from a given section of river; the data collected represented the average of data from good ensembles from a dwell location. The metric, instead, points out locations in the river where the ADCP may be adversely affected by high-velocity or high-turbulence flow conditions requiring longer data collection.

3.4. Comparison of ADCP and Pitot Tube Data

[42] Figure 8 shows the mean velocity measured by the pitot tube (0.39 m below the surface) and the mean velocity of the upper bin (1.55 m below the surface) measured by the ADCP for flow at rapid 13. Values measured with each instrument appeared to be comparable in the upper pool. As the flow accelerated into the main section of rapid 13, the magnitude of velocity recorded by each instrument rose in unison until a position near 300 m, whereupon velocity measurements diverged. While peak ADCP velocities were grouped around 3.0 m/s from 300 to 700 m, the pitot tube data indicated the velocities at 0.39 m below the surface were closer to 4.0 m/s.

[43] One possible explanation of the difference in measured velocities between instruments is that one or both instruments misread the velocities in the flow. While both instruments have been tested and qualified at high velocity [*RDInstruments*, 1996; *Eberhard*, 1997; *Yorke and Oberg*, 2002], turbulent flow conditions in rapids may create issues with accuracy. The pitot tube reads a pressure difference between two ports, has been designed to operate in fast water, and presumably measures high-velocity flow with accuracy. Over a decade of working measurements on high-velocity rivers and streams in New Zealand adds to the confidence that the pitot tube accurately recorded the high velocities. The ADCP, in theory, should be able to measure flow up to 10 m/s. Given the theory of operation of the instrument, however, it is possible the ADCP may have underestimated flow speed in the rapid. The ADCP experienced some data loss in fast water. If the dropped ADCP data were from higher-velocity regions or high-velocity fluctuations, the averaged velocity from the remaining measured data might underestimate the actual flow magnitude. Nonetheless, it is also possible the differences in velocity illustrated by Figure 8 represent real flow behavior in the rapids. The ADCP bin 1 was 1.55 m below the water surface while the pitot tube was 0.39 m below the water surface. Because it was positioned over a meter higher in the water column, the greater velocities reported by the pitot tube may reflect faster flow near the water surface. To test this hypothesis, the flow structures from closely aligned pitot tube and ADCP measurements were analyzed.

[44] Figure 9 shows the velocity profile from four different locations at rapid 13 where both ADCP and pitot tube measurements were made. These four locations were chosen because of the proximity of the ADCP and pitot tube data. In each of the four locations, a pitot tube measurement was made within 6 m of the ADCP location. In the upper pool, the ADCP measured a velocity profile that is typical of prismatic, rough-boundary rivers, and ADCP and pitot tube measurements appeared to agree. In the tongue of the rapid, the velocity away from the bed reached a relatively uniform velocity of 3.0 m/s in the upper four bins by the ADCP. The pitot tube measurement at this location was roughly 3.6 m/s, a speed that was out of alignment with the profile measured by the ADCP. The next point downstream in Figure 9 was in

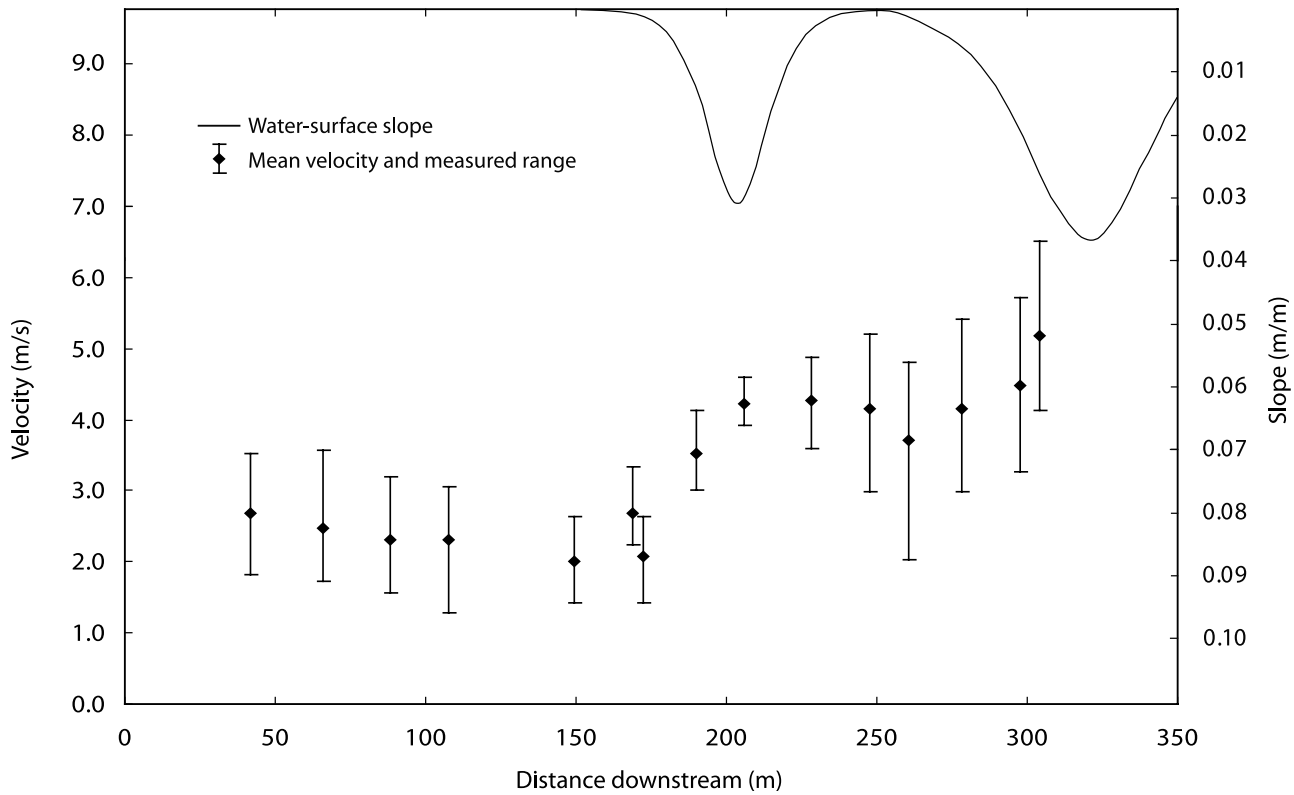

Figure 7. Mean velocity at rapid 21 measured using the pitot-static tube; water surface slope is also displayed to show the location of the constrictions. The tongue of the leading riffle was located at a downstream distance of about 210 m, and the tongue of the main rapid was located near 300 m. Error bars on the velocity data show the range of instantaneous velocities recorded by the pitot tube during a given measurement. The fastest mean velocity recorded in the tongue of the main rapid was 5.2 m/s; the largest recorded instantaneous velocity was 6.5 m/s.

the core of the rapid below the first breaking waves of the tongue. The velocity profile recorded by the ADCP was unusual with a large velocity near the bed, minimum velocities values in the second and third bins from the bottom and flow linearly increasing with height toward the surface. When plotted on the same graph, the single pitot tube measurement fell in line with the trends of the velocity profile captured by the ADCP. Finally, the comparison of ADCP

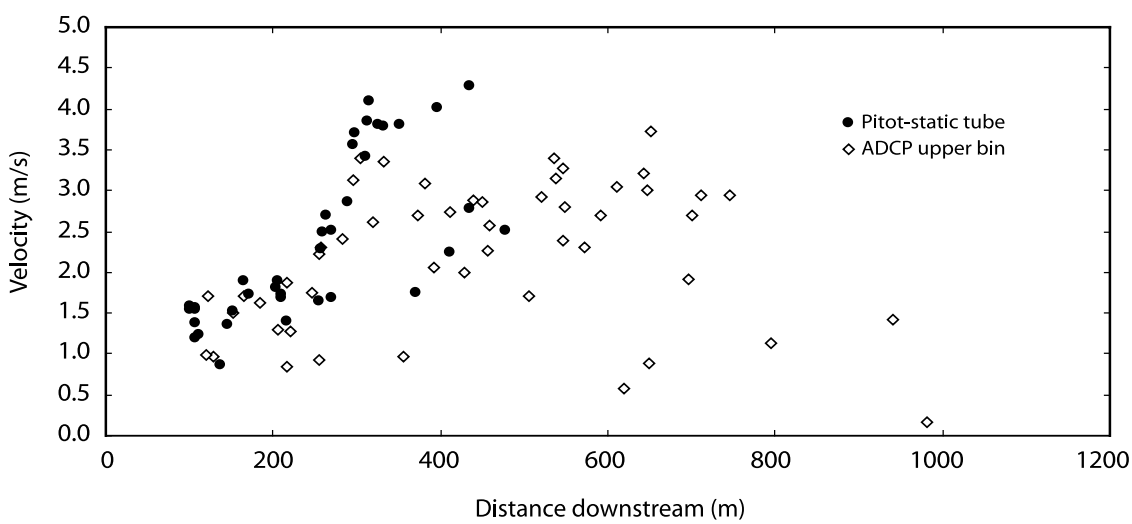

Figure 8. Comparison of near-surface velocity data at rapid 13. The pitot tube data were measured 0.39 m below the surface, and the ADCP bin 1 data were located 1.55 m below the surface. The first breaking waves of the rapid were located at a downstream distance of 330 m. Agreement between instruments was good in the upper pool and tongue. Instrument values began to diverge below the first breaking waves, with ADCP data indicating slower flow and pitot tube data indicating faster flow for another 100 m.

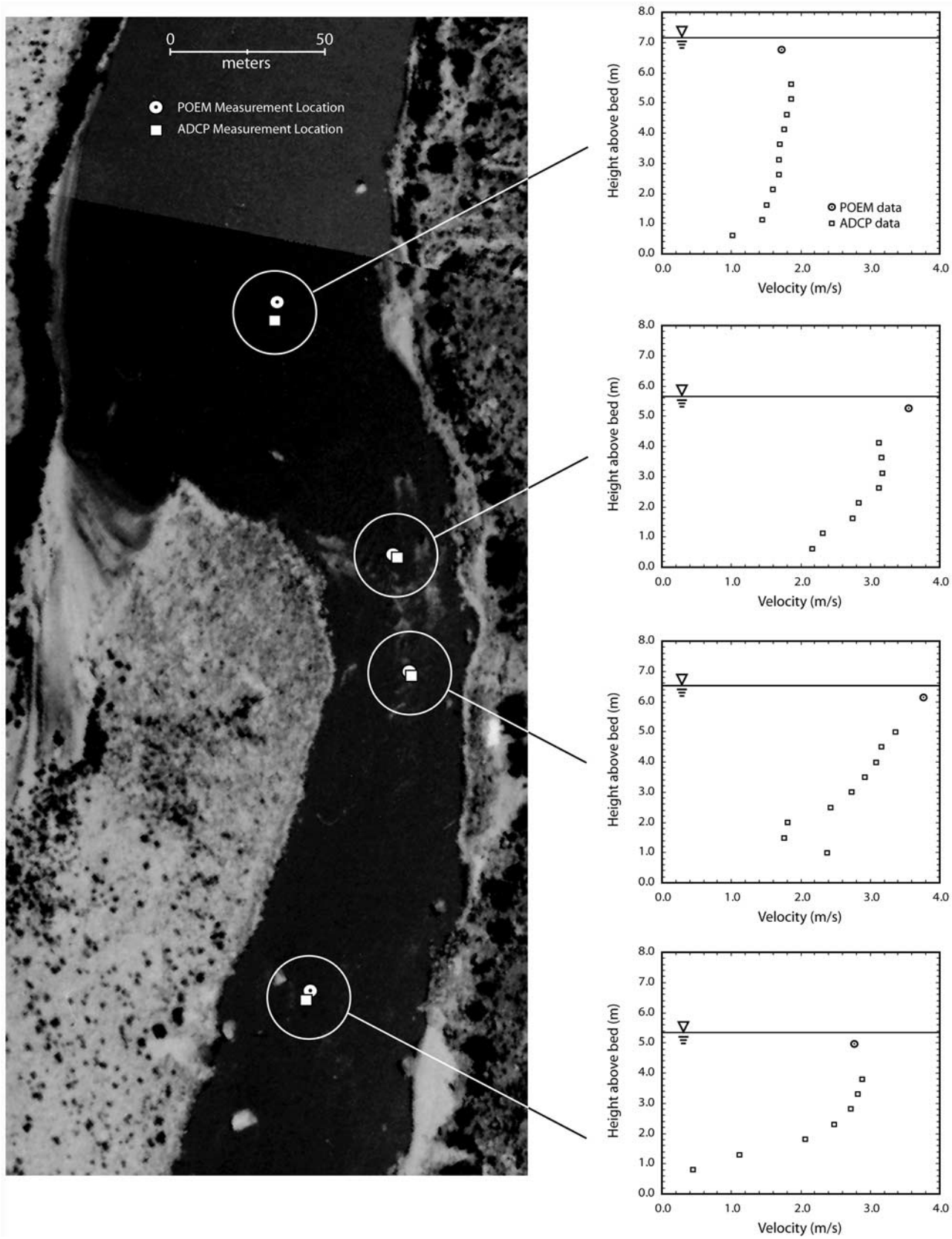

Figure 9. Velocity profiles at four locations in rapid 13 comparing the ADCP data (squares) and the pitot tube data (circles).

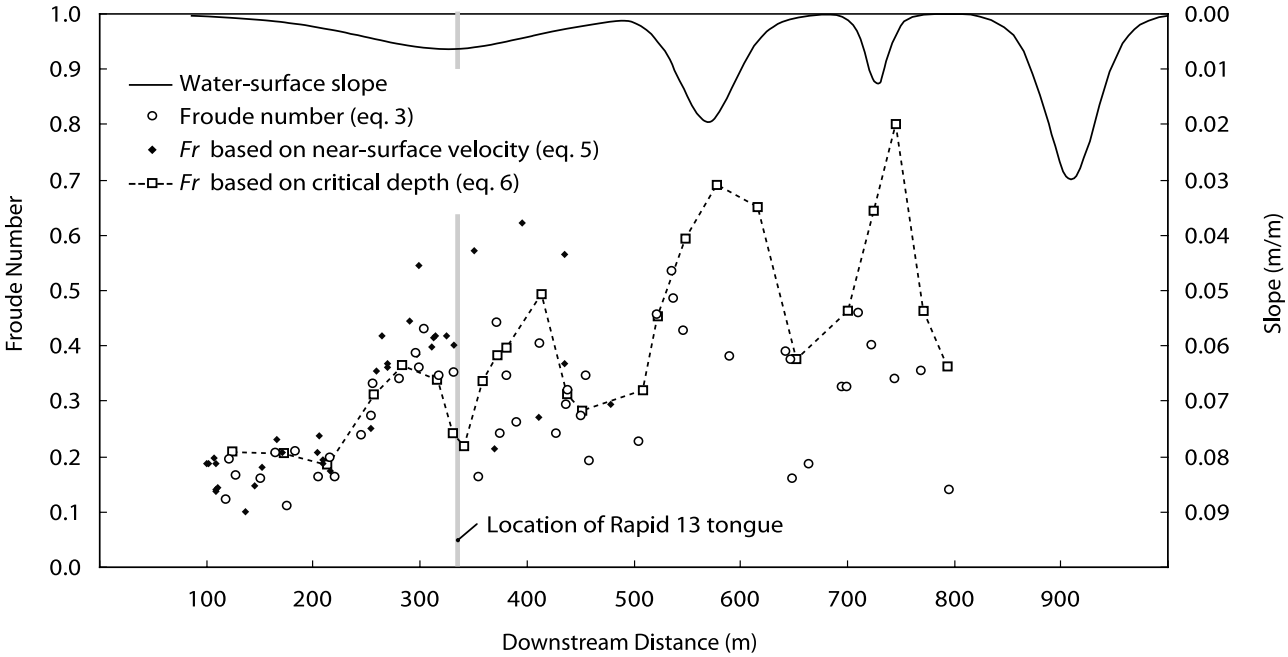

Figure 10. Froude numbers at rapids 13 and 14 show subcritical flow. In the tongue of rapid 13, *Fr* calculated using near-surface velocity (equation (5)) shows good agreement with *Fr* calculated with the standard equation (equation (3)) using water velocity data from throughout the water column. The data in the upper pool and the tongue of the rapid also compare well with *Fr* calculated on the basis of critical depth (equation (6)). For reference, the location of the tongue of rapid 13 is indicated with the vertical gray line. Downstream of the tongue of rapid 13, the estimates of Froude number using the three techniques are poorly correlated.

data and the pitot tube measurement in the tailwaves below the rapid indicated good alignment between the two data sets. The data in Figure 9 seem to suggest both instruments were measuring real flow behavior in the rapid in a complimentary fashion. More importantly, within the core of the rapid, the data suggest the highest velocity occurred near the water surface. *Tinkler* [1997] observed similar velocity profiles in near-critical flow conditions and suggested that in high-gradient, rough rivers, the upper part of the water profile can shear over the lower part of the profile.

3.5. Froude Number

[45] ADCP and bathymetry data collected at rapids 13 and 14 permitted calculation of *Fr* with equation (3). The efficacy of applying equation (5) was also evaluated at rapid 13 using available data from all instruments. At rapid 21, ADCP data were not collected and *Fr* was calculated with equation (5) using pitot tube data measured near the water surface and depths collected with the fathometer.

[46] Plotted in Figure 10 with water surface slope to illustrate the location of rapids, *Fr* was consistently less than 0.3 in the upper pool above rapid 13. *Fr* increased to a maximum value of 0.4 as flow accelerated into rapid 13. *Fr* then decreased in the downstream direction before again increasing to 0.5 in the accelerated flow of rapid 14; *Fr* again increased to nearly 0.5 in the secondary rapid below rapid 14. The flow remained subcritical throughout each rapid, never approaching critical flow conditions. Figure 10 shows *Fr* reached a maximum value at the smooth water just upstream of the first breaking waves of a given rapid. This finding is consistent with the postulate that maximum *Fr* occurs at the location of the greatest constriction in a river, where velocity is greatest and the depth is at a minimum. While the fastest flow in rapid 13 was not directly measured because of safety concerns, as discussed earlier, these flow velocities were not appreciably faster than the measured flow, and *Fr* was probably not much larger than 0.4 reported above.

[47] The necessary condition of hydrostatic pressure distribution when calculating *Fr* using shallow-water theory is likely valid in the upper pool, and probably valid in the tongue of the rapid. In the core of the rapid, particularly just downstream of the first breaking waves, the hydrostatic assumption may begin to break down. According to *Henderson* [1966, p. 28], a river is considered very steep if the slope is above 0.01, implying the hydrostatic assumption remains valid up to that gradient. In the current study, the peak slope in rapid 13 was 0.006 and the peak slope of rapid 14 was 0.02. While rapid 14 can be classified as steep, the slope in water surface is not greatly different from that threshold where the hydrostatic assumption is still valid. Any slope-induced hydrostatic error would be small and probably not greater than errors inherent in the flow velocity measurements.

[48] Values of *Fr* calculated using just surface velocity and water depth (equation (5)) are also shown in Figure 10. Values of velocity distribution coefficient, β, calculated with ADCP data in rapid 13 and rapid 14 showed β ranged from 1.00 to 1.12, and the average value was 1.06. This average value of $\beta = 1.06$ was used for all calculations of *Fr* using equation (5). *Fr* calculated with just near-surface velocity and water depth showed good agreement with the *Fr* data calculated with equation (3) in the upper pool and tongue

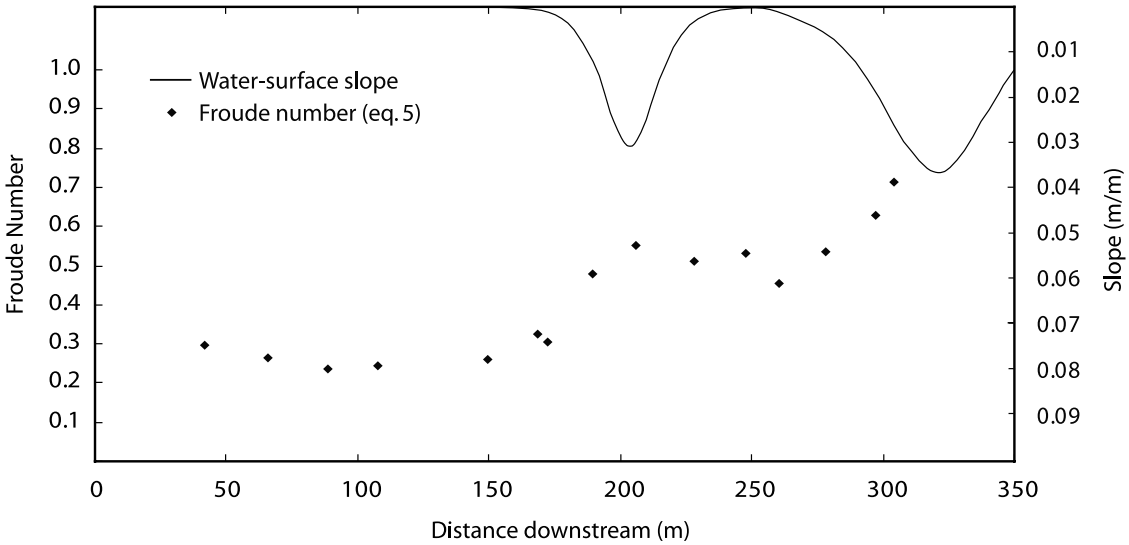

Figure 11. Froude number at rapid 21 as calculated using near-surface velocity and the depth of flow at the particular location. Froude number is largest in the fast, smooth water just upstream of the breaking waves of the main rapid.

of the rapid. Estimates of *Fr* from equation (5) in the core of the rapid, downstream of the first breaking waves, diverged from the value of *Fr* from equation (3). The higher velocity measured with the pitot tube near the water surface, caused these elevated values of *Fr*. Equation (5) overestimates *Fr* in the core of the rapid downstream from the first breaking waves and should not be used in the core of the rapid owing to the high surface velocity relative to mean velocity at depth.

[49] Another potential error source in calculating *Fr* with equation (3) and ADCP data alone is the inability of the ADCP to measure surface velocity directly. The top bin of the ADCP measurements was 1.55 m below the water surface and data in this study indicated velocity at the surface could be greater than velocity at 1.55 m depth, particularly in the core of a rapid. Therefore, *Fr* calculations in the core of the rapid using ADCP data may tend to underestimate actual *Fr*, though this error is probably less than 10% and decreases in deeper flow where more ADCP data can be collected.

[50] To test the validity of the values of *Fr* calculated with depth-integrated velocity and near-surface velocity (i.e., equations (3) and (5)) for rapid 13, *Fr* was also calculated using the one-dimensional approach of equation (6). This equation is not a true calculation of *Fr* at a given point and could differ significantly from the true values calculated with equation (3), but the equation does offer, using unique data of bathymetry and not flow velocity, a rough estimate of what *Fr* should be in any section of the river. This technique was applied to the section of the river leading into rapid 13 (Figure 10). Froude number calculated using equation (6) agreed well with the *Fr* data calculated using velocity both in the pool above the rapid and in the section of greatest constriction located at a downstream distance of about 280 m. The *Fr* at 280 m, using equation (6), was calculated to be 0.37. More telling, the critical depth of flow at this location was calculated to be 3.5 m while the actual flow depth in the river at the time of measurement was 5.5 m. Farther downstream, the critical depth gets closer to the true water surface, exemplified by the gradually rising *Fr*, but all flow in the channel remains subcritical. Similarly, *Schmidt* [1990], using the approach of equation (6) and bathymetric data from Badger Rapid (a sizable rapid on the Colorado River in Grand Canyon), reported a maximum *Fr* = 0.6.

[51] Froude numbers at rapid 21, calculated with equation (5), are shown in Figure 11. Closely tracking the near-surface velocity leading into the rapid (Figure 7), *Fr* was roughly 0.2 in the pool above the rapid before increasing to 0.5 at the first riffle of rapid 21. As flow was accelerated into the main section of the tongue of rapid 21, *Fr* increased to 0.7 just upstream of the first breaking waves of rapid 21. Because detailed bathymetric data were not available, equation (6) could not be used at rapid 21.

[52] Though it is possible errors in the velocity or bathymetry measurements might have led to an under prediction in *Fr* in this study, errors in velocity are probably below 20% and error in bathymetry is probably less than 5%. As such, even considering measurement error, it is unlikely that *Fr* in rapids 13, 14, or 21 is supercritical. Furthermore, calculation of the critical depth using equation (6) confirms subcritical flow in rapids 13 and 14. While threads of faster, supercritical flow [*Tinkler*, 1997] were observed at the water surface near breaking waves, reported *Fr* values in this study were depth integrated (equations (3) and (5)) or channel wide (equation (6)) and indicated subcritical flow throughout each rapid.

3.6. Breaking Waves and the Nature of Critical Flow in Rapids

[53] One of the arguments that flow in large rapids is supercritical is the presence of specific wave patterns on the water surface. It has been suggested, for example, that stationary, nonbreaking waves in the tongues of rapids, like those waves in rapid 21 measured in this study, are undular hydraulic jumps indicating *Fr* = 1.0–1.7 [*Kieffer*, 1990]. Undular hydraulic jumps, however, exhibit an elevated water surface and reduced water velocity downstream from the jump. But the measured water velocity in the rollers of rapid 21 showed flow was subcritical (Figure 11). Also, there was no elevated water surface and decelerated flow

downstream of the rollers indicative of an undular hydraulic jump. Rollers in the tongue of rapids are not undular jumps, instead, they are standing waves produced in near-critical flow by depth perturbations on the bed of the channel [see *Henderson*, 1966, p. 45].

[54] Similarly, breaking normal waves in the Colorado River have been taken as evidence of supercritical flow. Fundamentally, a breaking wave indicates that the disturbance creating the wave results in wave propagation speed less than the surface velocity entering the wave (i.e., *Fr*, the ratio of inertial to gravitational forces, is larger than 1.0). Thus, the wave breaks upon itself to maintain the wave position within the flow. On the basis of the work of hydraulic jumps for one-dimensional flow in flumes, waves begin to break at *Fr* of about 2 [see *Henderson*, 1966, pp. 215–218]. A direct comparison of flume studies with the highly turbulent and broken surface of the larger waves found in rapids suggests *Fr* could be as large as 3–9 at the water surface [see also *Chow*, 1959, p. 395]. But breaking normal waves in rapids, while indicating localized surface conditions of supercritical flow [*Tinkler*, 1997], do not necessarily point to supercritical flow throughout the water column or across the expanse of the channel. Consistent with the findings of *Tinkler* [1997], the results of this study show these regions of breaking waves, or threads of supercritical flow, are confined to narrow, shallow sections near the water surface. When the entire depth of the channel is integrated into *Fr* calculation, it becomes apparent that flow in rapids is critical or subcritical. As discharge increases, assuming the rapid does not drown out, the spatial extent of depth-integrated critical flow can expand [*Tinkler*, 1997], but depth-integrated flow in rapids is generally not supercritical, even during large floods.

[55] True supercritical flow affecting the entire channel of a river near a rapid would have hydraulic characteristics quite different than the flow patterns observed in Colorado River rapids. Debris fans create constrictions in the channel that can force critical flow, but if flow downstream from the constriction forming the rapid were supercritical, the streamlines of the flow exiting the constriction would diverge to fill the channel until a hydraulic jump spanning the width of the channel returned the flow to subcritical. This flow behavior has been demonstrated in flumes [*Chow*, 1959; *Carling*, 1995] and observed in bedrock channels [*Carling*, 1995] and is distinctly different than flow behavior observed in rapids of the Colorado River. *Schmidt et al.* [1993, p. 2931], who modeled a debris flow constriction and rapid in a flume, showed that in supercritical flow ($Fr \sim 2$), streamlines diverge downstream from the constriction before the flow experiences a pronounced hydraulic jump. The experiments of *Schmidt et al.* [1993] also showed that in transcritical flow, any hydraulic jump is confined to the constriction, consistent with observations in actual rapids. Because the Colorado River flows over coarse-grained alluvium at all rapids [*Hanks and Webb*, 2006], the channel adjusts to rising discharge, achieving critical flow conditions at the debris-fan constrictions of rapids [*Kieffer*, 1985]. However, there is no compelling evidence to suggest that channel-scale flow in debris-fan rapids on the Colorado River goes supercritical, even at large discharge. This observation is important in studies of the hydraulics and fluvial geomorphology of the Colorado River and its tributaries because it allows researchers and engineers to bracket the flow conditions that could be expected, even at large discharge.

4. Conclusions

[56] Velocity, bathymetry, and water surface measurements were made in rapids on the Colorado River in Cataract Canyon, Utah. These boat-based measurements offer insight into the complicated hydraulics of rapids and help evaluate some assumptions applied to analysis of the high-velocity water flowing in high-gradient rivers.

[57] The collection of detailed bathymetric and water surface data near and downstream of rapid 13 showed the complete topographic domain of the water within these rapids. The data revealed the three-dimensional nature of the water surface in rapids indicating water surface elevations along the shoreline of a rapid can misrepresent the actual slope of the rapid in the channel. Collection of these data is also an early step in building computational fluid dynamic models to simulate flow in rapids.

[58] Two flow-measurement instruments, an electronic pitot-static tube and an ADCP, were used to characterize the flow fields in three rapids. Both instruments proved valuable during the study, each offering unique advantages for collecting velocity data in the challenging conditions of high-gradient rivers. The pitot tube, placed just below the water surface, collected detailed velocity data, including the range of turbulent fluctuations in the flow. Maximum mean velocity measured with the pitot tube was 5.2 m/s and the fastest instantaneous velocity was 6.5 m/s. The pitot tube design proved well suited to measurements in the high-velocity flow field of the rapid. The ADCP collected flow data throughout much of the water column and operated successfully within fast sections of water, though some data suggested the possibility that the ADCP may underestimate velocity of the fastest flow. The ADCP recorded mean velocities as high as 3.7 m/s.

[59] In contrast to the flow in alluvial rivers where the point of maximum velocity is located below the surface, it appeared the highest velocity in the core of rapids (i.e., below the first breaking waves) was forced to the water surface, though further work is needed to confirm or discount this observation. The ADCP provided valuable and reliable bathymetric data from slow and fast sections of the river. Using a new approach of preserving the depth measurements from each beam in an ensemble, detailed bathymetric maps of the river bed were constructed.

[60] Froude number calculations indicated flow was subcritical in the moderately sized rapids and did not exceed critical conditions even in the large rapid. Breaking waves were observed even though the overall channel flow conditions remained subcritical. For the flow conditions analyzed, the largest *Fr* measured was 0.7 in the tongue of rapid 21. The study indicated *Fr* reached a maximum at the tongue of a given rapid, decreasing below the first breaking waves. Realistic estimates of *Fr* in rapids were obtained using only near-surface water velocity and water depth. With the *Fr* data from this current study, comparisons with flow conditions of earlier studies in rapids led us to conclude that supercritical flow in the rapids of the Colorado River is rare and that channel-scale flow conditions in rapids remain subcritical or critical even at large discharge.

[61] **Acknowledgments.** We are indebted to Peter Griffiths for tacheometric support, Steve Young for skilled and safe navigation of the boat in the rapids, Steve Cunningham for robust engineering of the boom assembly, and Terry Kenney for collecting ADCP data in the river. Jim Liggett provided insight into the specifics of critical flow and calculating Froude number. Mike Nolan and Bill Knight provided early reviews of the manuscript, and the insightful comments from three anonymous reviewers greatly improved the final article.

References

Ackerman, J. D., and T. M. Hoover (2001), Measurement of local bed shear stress in streams using a Preston-static tube, *Limnol. Oceanogr.*, *46*(8), 2080–2087.

Belknap, B., B. Belknap, and L. Belknap Evans (2006), *Belknap's Waterproof Canyonlands River Guide*, 75 pp., Westwater, Evergreen, Colo.

Best, J. L., and A. G. Roy (1991), Mixing-layer distortion at the confluence of channels of different depth, *Nature*, *350*(6317), 411–413, doi:10.1038/350411a0.

Blalock, M. E., and T. W. Sturm (1981), Minimum specific energy in compound open channel, *Proc. Am. Soc. Civ. Eng.*, *107*(6), 699–717.

Carling, P. A. (1995), Flow-separation berms downstream of a hydraulic jump in a bedrock channel, *Geomorphology*, *11*(3), 245–253, doi:10.1016/0169-555X(94)00052-S.

Chow, V. T. (1959), *Open-Channel Hydraulics*, 680 pp., McGraw-Hill, New York.

Costa, J. E., K. R. Spicer, R. T. Cheng, P. Haeni, N. B. Melcher, E. M. Thurman, W. J. Plant, and W. C. Keller (2000), Measuring stream discharge by non-contact methods: A proof-of-concept experiment, *Geophys. Res. Lett.*, *27*(4), 553–556, doi:10.1029/1999GL006087.

De Serres, B., A. D. Roy, P. M. Biron, and J. L. Best (1999), Three-dimensional structure of flow at a confluence of river channels with discordant beds, *Geomorphology*, *26*, 313–335, doi:10.1016/S0169-555X(98)00064-6.

Douglas, M. E., and P. C. Marsh (1996), Population estimates/population movements of *Gila cypha*, an endangered cyprinid fish in Grand Canyon region of Arizona, *Copeia*, *1*, 15–28, doi:10.2307/1446938.

Eberhard, A. (1997), POEM test certificate dated 30 October 1997/EA, Swiss Natl. Hydrol. and Geol. Surv., Bern, Switzerland.

Fox, R. W., and A. T. McDonald (1985), *Introduction to Fluid Mechanics*, 741 pp., John Wiley, New York.

Grams, P. E., and J. C. Schmidt (1999), Geomorphology of the Green River in the eastern Uinta Mountains, Dinosaur National Monument, Colorado and Utah, in *Varieties of Fluvial Form*, edited by A. J. Miller and A. Gupta, pp. 81–111, John Wiley, Chichester, U. K.

Grant, G. E. (1997), Critical flow constraints flow hydraulics in mobile-bed streams: A new hypothesis, *Water Resour. Res.*, *33*(2), 349–358, doi:10.1029/96WR03134.

Hanks, T. C., and R. H. Webb (2006), Effects of tributary debris on the longitudinal profile of the Colorado River in Grand Canyon, *J. Geophys. Res.*, *111*, F02020, doi:10.1029/2004JF000257.

Hazel, J. E., Jr., D. J. Topping, J. C. Schmidt, and M. Kaplinski (2006), Influence of a dam on fine-sediment storage in a canyon river, *J. Geophys. Res.*, *111*, F01025, doi:10.1029/2004JF000193.

Henderson, F. M. (1966), *Open Channel Flow*, 522 pp., Macmillan, New York.

Howard, A., and R. Dolan (1981), Geomorphology of the Colorado River in Grand Canyon, *J. Geol.*, *89*, 269–298.

Jarrett, R. D. (1984), Hydraulics of high-gradient streams, *J. Hydraul. Eng.*, *110*(11), 1519–1539, doi:10.1061/(ASCE)0733-9429(1984)110:11(1519).

Kieffer, S. W. (1985), The 1983 hydraulic jump in Crystal Rapid: Implications for river-running and geomorphic evolution in the Grand Canyon, *J. Geol.*, *93*, 385–406.

Kieffer, S. W. (1987), The waves and rapids of the Colorado River, Grand Canyon, *U.S. Geol. Surv. Open File Rep.*, *87-096*, 69 pp.

Kieffer, S. W. (1988), Hydraulic map of Lava Falls Rapid, Grand Canyon, Arizona, *U.S. Geol. Surv. Misc. Invest. Ser. Map*, *I-1897-J*, scale 1:1,000, 1 sheet.

Kieffer, S. W. (1990), Hydraulics and geomorphology of the Colorado River in the Grand Canyon, in *Grand Canyon Geology*, edited by S. S. Bues and M. Morales, pp. 333–383, Oxford Univ. Press, New York.

Lane, S. N., P. M. Biron, K. F. Bradbrook, J. B. Butler, J. H. Chandler, M. D. Crowell, S. J. McLelland, K. S. Richards, and A. D. Roy (1998), Three-dimensional measurement of river channel flow processes using acoustic Doppler velocimetry, *Earth Surf. Processes Landforms*, *23*, 1247–1267, doi:10.1002/(SICI)1096-9837(199812)23:13<1247::AID-ESP930>3.0.CO;2-D.

Larsen, I. J., J. C. Schmidt, and J. A. Martin (2004), Debris-fan reworking during low-magnitude floods in the Green River canyons of the eastern Uinta Mountains, Colorado and Utah, *Geology*, *32*(4), 309–312, doi:10.1130/G20235.1.

Leopold, L. B. (1969), The rapids and the pools—Grand Canyon, in *The Colorado River Region and John Wesley Powell*, *U.S. Geol. Surv. Prof. Pap.*, 669, pp. 131–145.

Liggett, J. A. (1993), Critical depth, velocity profiles, and averaging, *J. Irrig. Drain. Eng.*, *119*(2), 416–422, doi:10.1061/(ASCE)0733-9437(1993)119:2(416).

Loomis, J., A. J. Douglas, and D. A. Harpman (2005), Recreation use values and nonuse values of Glen and Grand Canyons, in *The State of the Colorado River Ecosystem in Grand Canyon*, edited by S. P. Gloss et al., pp. 153–164, *U.S. Geol. Surv. Circ.*, *1282*.

Magirl, C. S. (2006), Bedrock-controlled fluvial geomorphology and the hydraulics of rapids on the Colorado River, Ph.D. dissertation, Univ. of Ariz., Tucson.

Magirl, C. S., P. G. Griffiths, and R. H. Webb (2006), ADV point measurements within rapids of the Colorado River in Grand Canyon, in *Examining the Confluence of Environmental and Water Concerns, Proceedings of the 2006 World Environmental and Water Resources Congress*, edited by R. Graham, 10 pp., doi:10.1061/40856(200)158, Am. Soc. of Civ. Eng., Reston, Va.

Magirl, C. S, G. M. Smart, J. W. Gartner, and R. H. Webb (2007), Techniques and instrumentation for measuring flow in high-gradient rivers, in *2007 Hydraulic Measurements & Experimental Methods Conference*, edited by E. A. Cowin and D. F. Hill, pp. 454–459, Am. Soc. of Civ. Eng., Reston, Va.

Melis, T. S., R. H. Webb, P. G. Griffiths, and T. J. Wise (1994), Magnitude and frequency data for historic debris flows in Grand Canyon National Park and vicinity, *U.S. Geol. Surv. Water Resour. Invest. Rep.*, *94-4214*.

Miller, A. J. (1994), Debris-fan constrictions and flood hydraulics in river canyons: Some implications from two-dimensional flow modeling, *Earth Surf. Processes Landforms*, *19*(8), 681–697, doi:10.1002/esp.3290190803.

Nikora, V. I., and G. M. Smart (1997), Turbulence characteristics of New Zealand gravel-bed rivers, *J. Hydraul. Eng.*, *123*(9), 764–773, doi:10.1061/(ASCE)0733-9429(1997)123:9(764).

Parker, G., and N. Izumi (2000), Purely erosional cyclic and solitary steps created by flow over a cohesive bed, *J. Fluid Mech.*, *419*, 203–238, doi:10.1017/S0022112000001403.

Rantz, S. E., et al. (1982), Measurement and computation of streamflow: Volume 1, Measurement of stage and discharge, *U.S. Geol. Surv. Water Supply Pap.*, *2175*, 284 pp.

RDInstruments (1996), Acoustic Doppler current profilers—Principles of operation: A practical primer, 54 pp., San Diego, Calif.

Roy, A. G., P. M. Biron, T. Buffin-Bélanger, and M. Levasseur (1999), Combined visual and quantitative techniques in the study of turbulent flows, *Water Resour. Res.*, *35*(3), 871–877, doi:10.1029/1998WR900079.

Schmidt, J. C. (1990), Recirculating flow and sedimentation in the Colorado River in Grand Canyon, Arizona, *J. Geol.*, *98*, 709–724.

Schmidt, J. C., and J. B. Graf (1990), Aggradation and degradation of alluvial sand deposits, 1965–1986, Colorado River, Grand Canyon National Park, Arizona, *U.S. Geol. Surv. Prof. Pap.*, 1493.

Schmidt, J. C., and D. M. Rubin (1995), Regulated streamflow, fine-grained deposits, and effective discharge in canyons with abundant debris fans, in *Natural and Anthropogenic Influences in Fluvial Geomorphology*, *Geophys. Monogr. Ser.*, vol. 89, edited by J. E. Costa et al., pp. 177–195, AGU, Washington, D. C.

Schmidt, J. C., D. M. Rubin, and H. Ikeda (1993), Flume simulation of recirculating flow and sedimentation, *Water Resour. Res.*, *29*(8), 2925–2939, doi:10.1029/93WR00770.

Smart, G. M. (1994), Turbulent velocities in a mountain river, in *Hydraulic Engineering '94: Proceedings of the 1994 Conference*, edited by G. V. Cotroneo and R. R. Rumer, pp. 844–848, Am. Soc. of Civ. Eng., Reston, va.

Smart, G. M. (1999), Turbulent velocity profiles and boundary shear in gravel bed rivers, *J. Hydraul. Eng.*, *125*(2), 106–116, doi:10.1061/(ASCE)0733-9429(1999)125:2(106).

Stevens, L. E., J. P. Shannon, and D. W. Blinn (1997), Colorado River benthic ecology in Grand Canyon, Arizona, USA: Dam, tributary and geomorphological influences, *Reg. Rivers Res. Manage.*, *13*, 129–149, doi:10.1002/(SICI)1099-1646(199703)13:2<129::AID-RRR431>3.0.CO;2-S.

Thompson, D. M. (2007), The characteristics of turbulence in a shear zone downstream of a channel constriction in a coarse-grained forced pool, *Geomorphology*, *83*, 199–214, doi:10.1016/j.geomorph.2006.05.001.

Thompson, D. M., E. E. Wohl, and R. D. Jarrett (1999), Velocity reversals and sediment sorting in pools and riffles controlled by channel constrictions, *Geomorphology*, *27*, 229–241, doi:10.1016/S0169-555X(98)00082-8.

Thorne, C. R., and L. W. Zevenbergen (1985), Estimating mean velocity in mountain rivers, *J. Hydraul. Eng.*, *111*(4), 612–624, doi:10.1061/(ASCE)0733-9429(1985)111:4(612).

Tinkler, K. J. (1997), Critical flow in rockbed streams with estimated values for Manning's *n*, *Geomorphology*, *20*, 147–164, doi:10.1016/S0169-555X(97)00011-1.

Trieste, D. J. (1992), Evaluation of supercritical/subcritical flows in high-gradient channel, *J. Hydraul. Eng.*, *118*(8), 1107–1118, doi:10.1061/(ASCE)0733-9429(1992)118:8(1107).

Valle, B. L., and G. B. Pasternack (2006), Field mapping and digital elevation modelling of submerged and unsubmerged hydraulic jump regions in a bedrock step-pool channel, *Earth Surf. Processes Landforms*, *31*, 646–664, doi:10.1002/esp.1293.

Webb, R. H. (1996), *Grand Canyon, a Century of Change*, Univ. of Ariz. Press, Tucson, Ariz.

Webb, R. H., P. T. Pringle, and G. R. Rink (1989), Debris flows from tributaries of the Colorado River, Grand Canyon National Park, Arizona, *U.S. Geol. Surv. Prof. Pap.*, *1492*, 39 pp.

Webb, R. H., T. S. Melis, P. G. Griffiths, and J. G. Elliot (1999), Reworking of aggraded debris fans, in *The Controlled Flood in Grand Canyon*, *Geophys. Monogr. Ser.*, vol. 110, pp. 37–51, AGU, Washington, D. C.

Webb, R. H., J. Belnap, and J. Weisheit (2004), *Cataract Canyon: A Human and Environmental History of the Rivers in Canyonlands*, 268 pp., Univ. of Utah Press, Salt Lake City, Utah.

Wilcox, A. C., and E. E. Wohl (2007), Field measurements of three-dimensional hydraulics in a step-pool channel, *Geomorphology*, *83*, 215–231, doi:10.1016/j.geomorph.2006.02.017.

Wohl, E. E., and D. M. Thompson (2000), Velocity characteristics along a small step-pool channel, *Earth Surf. Processes Landforms*, *25*, 353–367, doi:10.1002/(SICI)1096-9837(200004)25:4<353::AID-ESP59>3.0.CO;2-5.

Yanites, B. J., R. H. Webb, P. G. Griffiths, and C. S. Magirl (2006), Debris flow deposition and reworking by the Colorado River in Grand Canyon, Arizona, *Water Resour. Res.*, *42*, W11411, doi:10.1029/2005WR004847.

Yorke, T. H., and K. A. Oberg (2002), Measuring river velocity and discharge with acoustic Doppler profilers, *Flow Meas. Instrum.*, *13*, 191–195, doi:10.1016/S0955-5986(02)00051-1.

J. W. Gartner and R. H. Webb, U.S. Geological Survey, 520 North Park Avenue, Tucson, AZ 85719, USA.

C. S. Magirl, U.S. Geological Survey, 934 Broadway, Suite 300, Tacoma, WA 98402, USA. (magirl@usgs.gov)

G. M. Smart, National Institute of Water and Atmospheric Research, Box 8602, Christchurch, New Zealand.